

Photocrosslinking and Click Chemistry Enable the Specific Detection of Proteins Interacting with Phospholipids at the Membrane Interface

Jacob Gubbens,^{1,4} Eelco Ruijter,^{2,5} Laurence E.V. de Fays,^{2,6} J. Mirjam A. Damen,³ Ben de Kruijff,¹ Monique Slijper,³ Dirk T.S. Rijkers,² Rob M.J. Liskamp,² and Anton I.P.M. de Kroon^{1,7,*}

¹Chemical Biology and Organic Chemistry, Bijvoet Center for Biomolecular Research and Institute of Biomembranes, Utrecht University, Padualaan 8, 3584 CH Utrecht, The Netherlands

²Medicinal Chemistry and Chemical Biology, Utrecht Institute for Pharmaceutical Sciences, Utrecht University, Sorbonnelaan 16, 3584 CA Utrecht, The Netherlands

³Biomolecular Mass Spectrometry and Proteomics Group, Bijvoet Center for Biomolecular Research and Utrecht Institute for Pharmaceutical Sciences, Utrecht University, Sorbonnelaan 16, 3584 CA Utrecht, The Netherlands

⁴Present address: Department of Biochemistry and Molecular Biology, Oregon Health & Science University, Portland, OR 97239, USA

⁵Present address: Department of Organic and Inorganic Chemistry, VU University, Amsterdam, The Netherlands

⁶Present address: Federal Agency for Drugs and Health Products, Bruxelles, Belgium

⁷Present address: Membrane Enzymology, Bijvoet Center for Biomolecular Research and Institute of Biomembranes, Utrecht University, Utrecht, The Netherlands

*Correspondence: a.i.p.m.dekroon@uu.nl

DOI 10.1016/j.chembiol.2008.11.009

SUMMARY

New lipid analogs mimicking the abundant membrane phospholipid phosphatidylcholine were developed to photocrosslink proteins interacting with phospholipid headgroups at the membrane interface. In addition to either a phenylazide or benzophenone photoactivatable moiety attached to the headgroup, the lipid analogs contained azides attached as baits to the acyl chains. After photocrosslinking in situ in the biomembrane, these baits were used for the attachment of a fluorescent tetramethylrhodamine-alkyne conjugate or a biotin-alkyne conjugate using click chemistry, allowing for the selective detection and purification of crosslink products, respectively. Proteins crosslinked to the lipid analogs in inner mitochondrial membranes from *Saccharomyces cerevisiae* were detected and subsequently identified by mass spectrometry. Established interaction partners of phosphatidylcholine were found, as well as known integral and peripheral inner membrane proteins, and proteins that were not previously considered mitochondrial inner membrane proteins.

INTRODUCTION

Membrane proteins play a crucial role in many cellular processes, including cell signaling and membrane trafficking. Up to 30% of all open reading frames are predicted to encode integral membrane proteins (Wallin and von Heijne, 1998). In addition, there must be numerous peripheral membrane proteins, considering that lipid binding domains are among the most common domains found in the eukaryotic proteome (DiNitto et al., 2003). Nevertheless, membrane proteins are traditionally underrepresented in most proteomics studies, which is caused mainly by

low expression levels and unfavorable properties such as poor solubility (Blonder et al., 2004; Santoni et al., 2000). Therefore, new methodology is required for analysis of this class of proteins by proteomics techniques.

One approach to detect peripheral and integral membrane proteins takes advantage of their interaction with lipids, and involves the use of photoactivatable lipid analogs to perform crosslinking in situ in the biomembrane (Brunner, 1993). Upon ultraviolet irradiation (UV) activation, covalent bonds are formed with adjacent molecules, thereby labeling membrane proteins of interest. This method has been used successfully in combination with radiolabeling to detect membrane proteins interacting with for instance 3-trifluoromethyl-3-[¹²⁵I]phenyldiazirine-phosphatidylcholine (TID-PC) in vitro (Janssen et al., 2002), and [³H]cholesterol, [³H]phosphatidylcholine, and [³H]phosphatidylinositol, all containing a photoreactive diazirine moiety, in vivo (Thiele et al., 2000). Although in these studies the photoactivatable moiety was located in the hydrophobic and relatively inert interior of the biomembrane, other studies have reported successful crosslinking to peripheral membrane proteins using the short chain *N*-([¹²⁵I]iodo-4-azidosalicylamidyl)-1,2-dilauroyl-*sn*-glycero-3-phosphoethanolamine [¹²⁵I]-ASA-DLPE (Berman et al., 1994; Desneves et al., 1996; Gao and Bauerlein, 1987; Montecucco, 1988; Montecucco et al., 1988) in which the photocrosslinking moiety is attached to the phosphoethanolamine headgroup via an amide bond.

Recently, the nonradioactive analog of this probe, *N*-(4-azidosalicylamidyl)-1,2-dilauroyl-*sn*-glycero-3-phosphoethanolamine (ASA-DLPE, **1**), was used in a proteomics approach aimed at analyzing the proteome interacting with the lipid headgroups (Gubbens et al., 2007). The probe was incorporated in inner mitochondrial membrane vesicles from the yeast *Saccharomyces cerevisiae* by addition from ethanolic solution. After photoactivation, carbonate wash, and separation of the proteins on SDS-PAGE, crosslinked proteins were visualized by measuring differences in UV absorbance, originating from the attached probe molecules. Two protein bands were found to contain

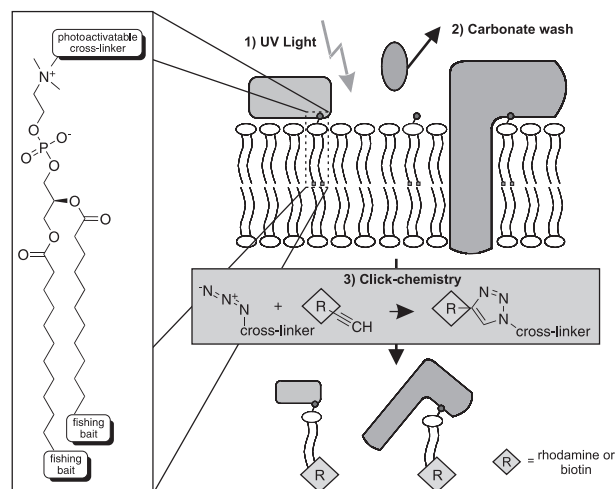


Figure 1. Outline of the Labeling Approach for Phospholipid-Interaction-Based Proteomics

A PC analog containing a photoactivatable headgroup and azides as fishing baits at the end of the acyl chains, is incorporated in a biological membrane. Photocrosslinking is performed, and noncrosslinked peripheral membrane proteins are washed away by carbonate. Subsequently the system is solubilized in 1% (w/v) SDS to attach a rhodamine or biotin reporter moiety (R) to the crosslink products for detection and purification, respectively.

crosslink products. Analysis by liquid chromatography-tandem mass spectrometry (LC-MS/MS) yielded a list of integral and peripheral membrane proteins that had potentially been crosslinked to ASA-DLPE. Although this study demonstrated the feasibility of photocrosslinking in detecting the phospholipid-interacting proteome, it suffered from two limitations. First, the detection by UV absorbance was not specific because proteins containing heme or flavin also produced a signal. Second, the presence of a large excess of uncrosslinked proteins complicated the identification of proteins that were crosslinked.

To eliminate these shortcomings, we developed novel lipid analogs (**3** and **4**) containing azides as fishing baits attached to short C11 lipid acyl chains that could be added to biological membranes from ethanolic solution. Azides are small and relatively apolar moieties, and therefore not expected to disturb the packing of the lipid bilayer. After photoactivation, carbonate wash, and solubilization of the membranes, they can be used for the covalent attachment of an alkyne-conjugated tag for visualization or affinity purification (Figure 1). The chemoselective reaction employed, a Cu(I)-catalyzed 1,3-dipolar cycloaddition commonly referred to as click chemistry (Rostovtsev et al., 2002; Tornøe et al., 2002), has proven a reliable ligation method in proteomics studies because the utilized functionalities do not occur in biological systems and are inert under physiological conditions (Ballell et al., 2005; Chan et al., 2004; Kuhlmann et al., 2002; Salisbury and Cravatt, 2007; Speers and Cravatt, 2004). The novel probes were designed to mimic phosphatidylcholine, the most abundant phospholipid in most eukaryotes, with the photoreactive group attached directly to the quaternary ammonium moiety of the headgroup. Using rhodamine-alkyne and biotin-alkyne conjugates for detection and purification of crosslink products, respectively, the new lipid analogs were found to crosslink specific subsets of membrane proteins after

incorporation in inner mitochondrial membrane vesicles from *S. cerevisiae*. In addition to crosslinks to established integral and peripheral membrane proteins, crosslinks to proteins not previously described as membrane proteins in yeast were also found, indicating the potential of the new lipid analogs as tools for proteome analysis.

RESULTS

Design and Synthesis

Three possible photoreactive crosslinking moieties were considered for the new lipid analogs: a diazirine (**2**), a benzophenone (**3**) and a phenylazide (**4**) as shown in Figure 2A.

Phospholipid probe **2** was synthesized via a reductive amination of the aldehyde 3-(4-formylphenyl)-3-(trifluoromethyl)diazirine, synthesized by using previously reported methods (Delfino et al., 1993), with 1,2-dilauroyl-*sn*-glycero-3-phospho-ethanolamine (DLPE). The resulting lipid analog was subsequently methylated to obtain **2**. However, preliminary results showed that diazirine probe **2** did not establish significant crosslinking to proteins (data not shown), most likely due to the high reactivity of the transient carbene species generated by photoactivation, causing reaction with water.

Based on the retrosynthetic analysis of probes **3** and **4** (Figure 2B), the photoactivatable phosphocholine-like headgroup in **A** was constructed from a common precursor by alkylation of the tertiary amine in **B** with a photoreactive benzylic bromide (**10** or **11**, Figure 3) (Wang et al., 2004). Because of the sensitivity of the photoreactive functionalities, they were introduced in the final step of the synthesis. The required (*N,N*-dimethylamino)ethyl phosphate **6** for **B** was accessible from commercially available **5** (LeKim et al., 1979).

Thus, *sn*-glycerophosphocholine (**5**) was subjected to a monodemethylation reaction in the presence of 1,4-diazabicyclo[2,2,2]octane (DABCO) (Figure 3) (LeKim et al., 1979; Wang et al., 2004). Subsequent acylation of crude **6**, with the imidazolidine generated in situ from 1,1'-carbonyldiimidazole (CDI) and 11-azidoundecanoic acid **8** (prepared from commercially available 11-bromoundecanoic acid **7**), afforded the tertiary amine **9** in 34% overall yield over two reaction steps. Although the yield was moderate, this strategy afforded an advanced intermediate that would otherwise be much more difficult to synthesize in a very short reaction sequence (Hermetter et al., 1989). All attempts to improve the yield of this reaction (e.g., by changing the sequence of reactions or by using alternative acylation protocols) were not successful.

Next, tertiary amine **9** was alkylated with the appropriate photoreactive probes (**10** and **11**) as their benzylic bromides. The required benzylic bromide for the synthesis of phospholipid probe **3**, 4-(bromomethyl)benzophenone **10** is commercially available. The 4-azidobenzyl bromide **11** required for the synthesis of phospholipid probe **4** was synthesized by diazo transfer to 4-aminobenzyl alcohol **12** (Liu and Tor, 2003), and conversion of the resulting azido-alcohol into the corresponding bromide. Bromide **11** was obtained in a moderate yield of 41% with incomplete conversion.

Alkylation of tertiary amine **9** with the benzylic photoreactive probes **10** and **11** was unsuccessful using a previously reported procedure (Wang et al., 2004). However, it was found that

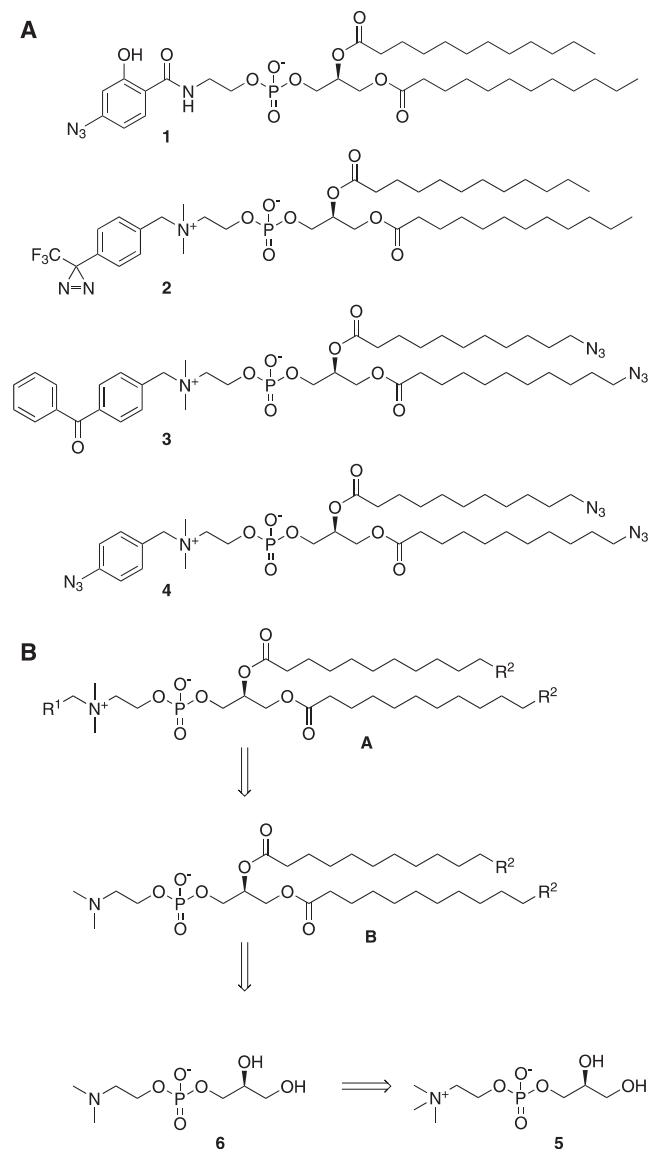


Figure 2. Structures and Retrosynthetic Analysis of the Photoactivatable Lipid Analogs

(A) Structures of ASA-DLPE (1), TPD-PC (2), benzophenone-PC (3), and phenylazide-PC (4).

(B) The retrosynthetic analysis of phospholipid analogs 3 and 4.

treatment of **9** with four equiv 4-(bromomethyl)benzophenone **10** in *N,N*-dimethylformamide (DMF) in the presence of 2,6-lutidine (2 equiv) as base under microwave irradiation (2 × 10 min at 120°C) led to complete conversion of the starting material to the desired photoprobe **3**. Under the same conditions, bromide **11** reacted smoothly with amine **9** to phospholipid probe **4**. Although thin-layer chromatography (TLC) analysis indicated a nearly complete conversion of the starting material, the isolated yields of photoprobes **3** and **4** were moderate, 45% and 60%, respectively, due to the formation of an unidentified side product with similar *R_f*-value that complicated purification by column chromatography. Purity and identity of the products were confirmed by TLC, ¹H and ¹³C NMR, and ESI-MS analysis.

Detection of Crosslinked Proteins in Model Membranes

Both benzophenone-PC (**3**) and phenylazide-PC (**4**) were first tested for their ability to crosslink to the peripheral membrane protein apo-cytochrome *c* in a model membrane system. Using the lipid analog ASA-DLPE (**1**), it was previously shown that crosslinking of this protein to membrane vesicles increased its carbonate wash-resistance (Gubbens et al., 2007). Large unilamellar vesicles obtained by extrusion technology (LUVET) were prepared containing 1,2-dioleoyl-*sn*-glycero-3-phosphocholine (DOPC), the anionic lipid 1,2-dioleoyl-*sn*-glycero-3-[phosphorac-(1-glycerol)] (DOPG) (7:3 mol/mol) to enhance the interaction with the basic apo-cytochrome *c*, and one of the new lipid probes (4 mol %). Apo-cytochrome *c* (0.12 mg/ml) was added to the LUVET (4 mM phospholipid) and a crosslink experiment was performed as described for ASA-DLPE (**1**) (Gubbens et al., 2007). After UV illumination at two different wavelengths, the vesicles were washed with carbonate, pelleted, and analyzed for associated apo-cytochrome *c* on SDS-PAGE gel using Coomassie staining (Figure 4). The results show an increase in the amount of apo-cytochrome *c* associated with the carbonate-washed vesicles after UV activation of the crosslinkers for 20 min. UV illumination at a wavelength of 254 nm was more effective in photoactivation than at 366 nm (compare lanes 3 and 5). Moreover, photoactivation of the phenylazide-PC probe (**4**) at 254 nm caused a smear above the protein band (lanes 3 and 4). A similar effect was observed previously for the ASA-DLPE probe (**1**), in which case the smear was found to contain crosslink products (Gubbens et al., 2007). For these reasons, 254 nm was selected as the preferred wavelength to perform crosslinking with both lipids.

Detection of Crosslinked Proteins in Biological Membranes

Next, the probes were incorporated in inner mitochondrial membrane vesicles (IMV) from the yeast *S. cerevisiae* by addition from a solution in ethanol, and their ability to crosslink to membrane proteins was tested. After crosslinking, the vesicles were washed with or without carbonate and solubilized in 1% (w/v) SDS to perform click chemistry. A tetramethylrhodamine (TAMRA)-alkyne conjugate (Invitrogen) was used as a fluorescent reporter. Proteins were isolated from the reaction mixture by precipitation, separated on SDS-PAGE gels, and scanned for fluorescence (Figure 5A). Both crosslinking with phenylazide-PC (**4**, lanes 1 and 2) and with benzophenone-PC (**3**, lanes 7 and 8) yielded multiple fluorescent protein bands. The intensity of most bands was unaltered by the carbonate wash, suggesting that the probes crosslink integral membrane proteins and/or peripheral membrane proteins that are rendered carbonate wash-resistant by the covalent linkage to the lipid probes. Strikingly, the two probes crosslink to different, albeit partially overlapping, subsets of proteins. The fluorescence signal observed for benzophenone-PC showed stronger resemblance to the Coomassie-stained pattern than that for phenylazide-PC (Figure 5B). In the absence of UV activation, the benzophenone-PC probe yielded more background fluorescence (lanes 9 and 10) than phenylazide-PC (lanes 3 and 4), of which the background signal was comparable to that obtained in the absence of crosslinker (lanes 11 and 12). The experiment was also performed using phenylazide-PC at a five times reduced concentration (Figure 5A, lanes

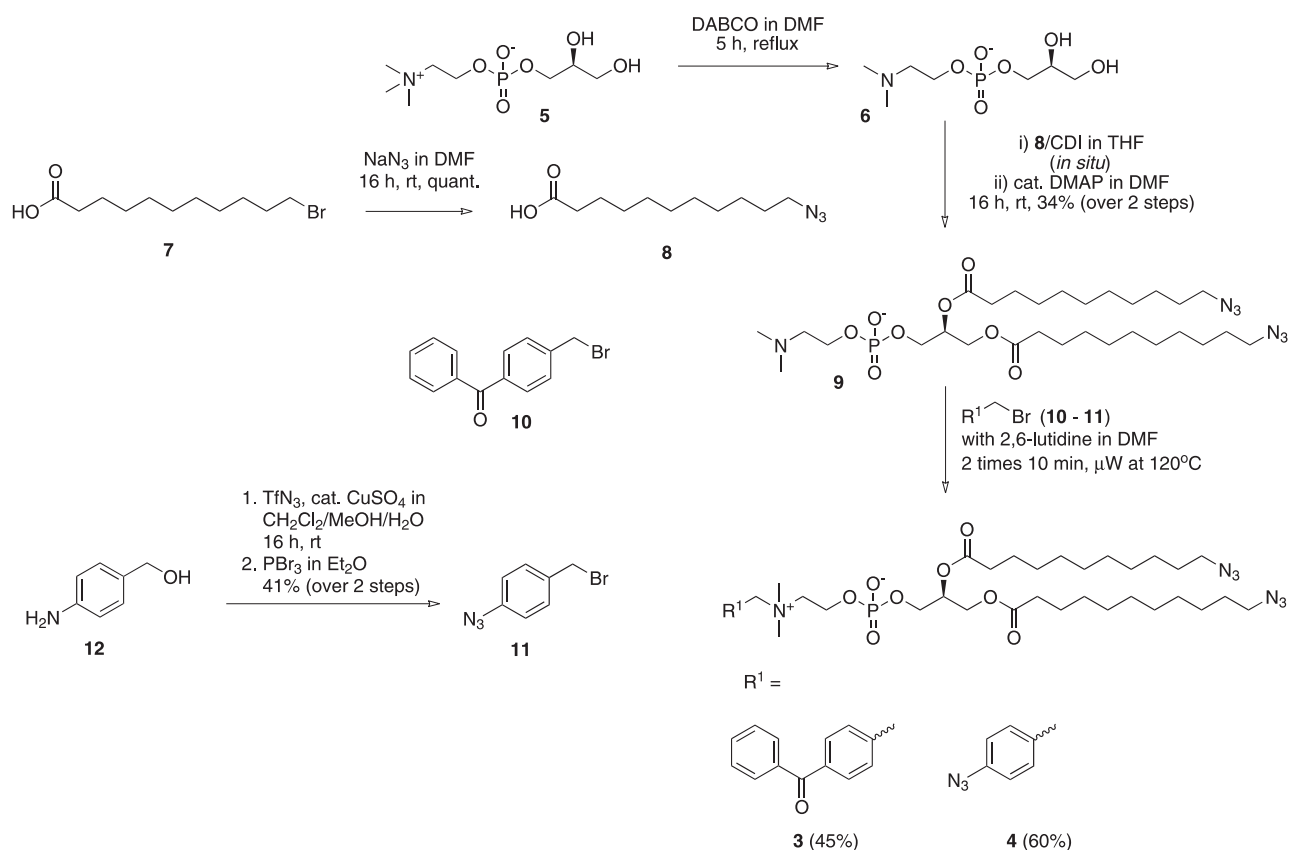


Figure 3. Synthesis of the Photoactivatable Phospholipid Probes 3 and 4

5 and 6). Labeling intensity was less, but the labeling pattern did not differ from that detected in lanes 1 and 2. Altogether, the data suggest that phenylazide-PC is the more suitable probe to identify proteins that are crosslinked in IMV.

Purification and Identification of Crosslinked Proteins

To identify the proteins crosslinked to phenylazide-PC (4) they were reacted with biotin-alkyne conjugate (Invitrogen) to enable purification on neutravidin beads. Biotinylation of crosslink products was confirmed by detection with a neutravidin-horseradish

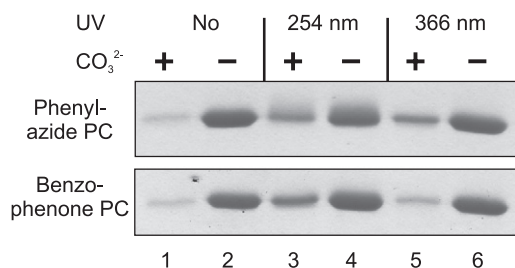


Figure 4. Crosslinking of Apo-Cytochrome c to Model Membranes LUVETs (DOPC/DOPG 7:3 [mol/mol] containing 4 mol % of the indicated crosslinker) were incubated with apo-cytochrome c (0.12 mg/mL). Crosslinking was performed at a lipid concentration of 4 mM using UV light of the indicated wavelengths for 20 min, and the vesicles were washed with or without carbonate. Apo-cytochrome c attached to the vesicles was precipitated, separated on SDS-PAGE, and stained with Coomassie.

peroxidase (HRP) conjugate on western blot (Figure 6A, lanes 1 and 2). The banding pattern obtained for the biotinylated proteins resembled the pattern for the fluorescently labeled proteins (compare lanes 1 and 2 of Figures 5A and 6A), although the resolution and dynamic range of the fluorescence detection method were much better. Neutravidin-HRP also bound to some proteins when no crosslinking had been performed (Figure 6A, lanes 3 and 4) or with no crosslinker present (lanes 5 and 6). The band at 250 kDa could be explained by the endogenously biotinylated mitochondrial protein Hfa1p (Hoja et al., 2004). In yeast mitochondria, no endogenously biotinylated proteins of smaller size are known. The prominent band at 35 kDa probably represents a protein to which the neutravidin-HRP conjugate binds aspecifically, because it did not bind to neutravidin beads during the purification of crosslinked proteins (Figure 6B, lane 2).

To purify crosslink products, proteins precipitated from the click chemistry reaction mixture corresponding to samples shown in lanes 1 and 3 of Figure 6A were dissolved by heating in 1% (w/v) SDS, and, after appropriate dilution, bound to neutravidin beads. Nonbiotinylated proteins were washed away, and the proteins of interest were eluted from the beads by heating in 2-fold concentrated SDS sample buffer. No biotinylated proteins could be detected when no crosslinking was performed, in contrast to the situation after crosslinking with phenylazide-PC (Figure 6B). The eluted proteins were separated on SDS-PAGE, digested, and identified by LC-MS/MS analysis (Table 1; see Table S1 available online for details on the protein

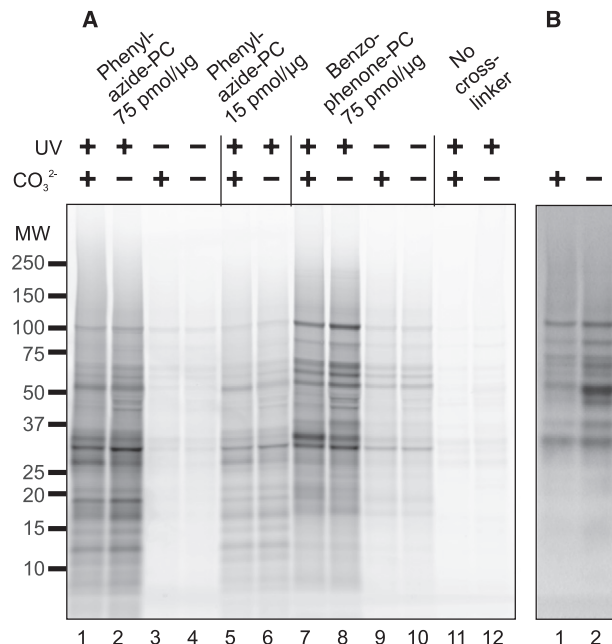


Figure 5. TAMRA Labeling of Crosslink Products from Mitochondrial Inner Membrane Vesicles

The indicated amounts of crosslinker per amount of mitochondrial protein were added from a solution in ethanol to IMVs from yeast mitochondria. The samples were either activated with UV light or left in the dark, and subsequently washed with or without carbonate, as indicated. Proteins were solubilized in 1% (w/v) SDS, subjected to click chemistry using a TAMRA-alkyne conjugate, and separated on a CRITERION XT 4%–12% (w/v) Bis-Tris gel (Bio-Rad) in MES running buffer. The gel was scanned for fluorescence (A) and subsequently stained with Coomassie (B). The Coomassie-stained pattern is shown only for lanes 1 and 2, because the other lanes showed corresponding banding patterns.

identifications). A total of 47 yeast proteins were found in the two samples, of which 37 are known mitochondrial proteins. A total of 27 proteins showed a significant increase (≥ 2 -fold) in the number of identified spectra after they were exposed to UV light in the presence of phenylazide-PC (4), and are therefore presumed to have been crosslinked by this lipid analog. A number of proteins was also detected in the absence of UV activation, which was attributed to aspecific binding to the neutravidin beads with the possible contribution of the unavoidable minute exposure of the sample to light. In comparison, LC-MS/MS analysis of the affinity-purified, biotinylated, crosslink products of benzophenone-PC (Table S2) demonstrated a significant increase in the number of identified spectra of 28 proteins, of which 13 were also found to be labeled by phenylazide-PC. This confirmed the interpretation of the fluorescence data in Figure 5 that the two probes crosslink to different, albeit overlapping, subsets of proteins.

DISCUSSION

In this study, we demonstrated that click chemistry is a convenient method to attach a tag to lipid-protein crosslink products for either fluorescence detection or affinity purification, thus allowing the unambiguous identification by LC-MS/MS of proteins

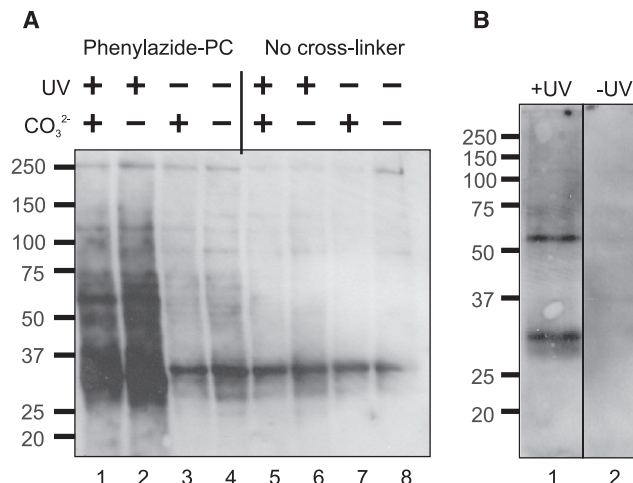


Figure 6. Biotin Labeling and Purification of Crosslink Products from Inner Membrane Vesicles

A crosslink experiment was performed in IMVs as described in the legend of Figure 5 using 75 pmol phenylazide-PC (4) per microgram mitochondrial protein, but instead of TAMRA, a biotin-alkyne conjugate was added via click chemistry. Samples were separated on gel, and proteins were transferred to a nitrocellulose membrane by western blotting. Biotinylated proteins were detected using a neutravidin-HRP conjugate (A). Samples corresponding to lane 1 (+UV) and lane 3 (–UV) were incubated with neutravidin beads in the presence of SDS. Proteins were eluted from the beads, separated on gel, and biotinylated proteins were detected as described above (B).

crosslinked to photoactivatable lipid analogs. Therefore, this method is a clear improvement over the approach described previously (Gubbens et al., 2007) to detect the phospholipid headgroup-interacting proteome.

Fluorescence detection of crosslinked proteins showed that benzophenone-PC (3) and phenylazide-PC (4) crosslink to distinct subsets of proteins that partially overlap. Some proteins are more efficiently or (almost) exclusively crosslinked by either phenylazide or benzophenone, whereas others show similar extents of crosslinking, which was confirmed by LC-MS/MS analysis of the biotinylated and affinity-purified crosslink products of both probes (Tables 1 and S2). The differences in labeling by the two probes probably reflect the different characteristics of the photoactivatable moieties. For instance, benzophenone has a preference to insert into C-H bonds (Dorman and Prestwich, 1994), whereas phenylazides often attack N-H bonds. Alternatively, the photoactivatable moieties might adopt different localizations at the membrane-water interface, exposing the probe molecules to amino acid residues that might differ in reactivity. In addition, the hydrophobic benzophenone moiety is larger than the phenylazide group, and therefore requires a larger binding pocket. Finally, the benzophenone moiety might render the membrane interface more hydrophobic, consistent with the observed decreased binding to benzophenone-PC containing LUVETs of cytochrome *c* (data not shown), which mainly interacts electrostatically with model biological membranes (Jordi and De Kruijff, 1996). In contrast, it was shown that apo-cytochrome *c*, which binds to the membrane due to exposed hydrophobic regions, binds and crosslinks equally well to vesicles containing either probe. In IMV, benzophenone-PC produced higher background fluorescence than phenylazide-PC, which might be

Table 1. LC-MS/MS Analysis of Phenylazide-PC Crosslink Products Purified on Neutravidin Beads

Protein Name	Open Reading Frame Name	Description	Molecular Weight (kDa)	Total no. of Identified Spectra		Location ^a
				+UV	–UV	
Lpd1	YFL018C	Dihydrolipoamide dehydrogenase component (E3) of the pyruvate dehydrogenase and 2-oxoglutarate dehydrogenase multienzyme complexes	54	11	1	M ^b
Gut2	YIL155C	Mitochondrial glycerol-3-phosphate dehydrogenase	72	13	4	M
Ndi1	YML120C	NADH:ubiquinone oxidoreductase, transfers electrons from NADH to ubiquinone in the respiratory chain but does not pump protons	57	12	4	Matrix ^c
Nop1	YDL014W	Nucleolar protein, component of the small subunit processome complex	34	3	1	N ^d
–	YDR119W-A	Putative protein of unknown function	7	3	1	Unknown
Lsc2	YGR244C	Beta subunit of succinyl-CoA ligase	47	3	1	M
Mrp7	YNL005C	Mitochondrial ribosomal protein of the large subunit	43	3	1	Matrix
Cor1	YBL045C	Core subunit of the ubiquinol-cytochrome c reductase complex (bc1 complex)	50	11	4	MIM ^e
Dld1	YDL174C	D-lactate dehydrogenase, oxidizes D-lactate to pyruvate	65	16	6	MIM
Nde1	YMR145C	Mitochondrial external NADH dehydrogenase	63	8	3	M
Cyt1	YOR065W	Cytochrome c1, component of the mitochondrial respiratory chain	34	13	5	MIM
Atp1	YBL099W	Alpha subunit of the F1 sector of mitochondrial F1F0 ATP synthase	59	10	4	MIM
Hhf1,2	YBR009C,YNL030W	Two identical histone H4 proteins	11	7	3	N
Cox2	Q0250	Subunit II of cytochrome c oxidase	29	4	2	MIM
Cox4	YGL187C	Subunit IV of cytochrome c oxidase	17	2	1	MIM
Atp17	YDR377W	Subunit f of the F0 sector of mitochondrial F1F0 ATP synthase	11	4	–	MIM
Ald4	YOR374W	Mitochondrial aldehyde dehydrogenase	57	4	–	M
Hta1,2	YDR225W,YBL003C	Nearly identical histone H2A subtypes	14	3	–	N
Lat1	YNL071W	Dihydrolipoamide acetyltransferase component (E2) of pyruvate dehydrogenase complex	52	3	–	M
Idh2	YOR136W	Subunit of mitochondrial NAD(+)-dependent isocitrate dehydrogenase	40	3	–	Matrix
Yme1	YPR024W	Subunit, with Mgr1p, of the mitochondrial inner membrane i-AAA protease complex	82	3	–	MIM
Chc1	YGL206C	Clathrin heavy chain, subunit of the major coat protein involved in intracellular protein transport and endocytosis	187	2	–	Endocytic vesicles
Phb2	YGR231C	Subunit of the prohibitin complex (Phb1p-Phb2p), a 1.2 MDa ring-shaped inner mitochondrial membrane chaperone	34	2	–	MIM
Atp2	YJR121W	Beta subunit of the F1 sector of mitochondrial F1F0 ATP synthase	55	2	–	MIM
Coy1	YKL179C	Golgi membrane protein with similarity to mammalian CASP	77	2	–	Golgi
–	YKR016W	Unknown protein, localized to the mitochondria	61	2	–	M
Lsp1	YPL004C	Long chain base-responsive inhibitor of protein kinases Pkh1p and Pkh2p	38	2	–	Eisosome
Qcr2	YPR191W	Subunit 2 of the ubiquinol cytochrome c reductase complex	40	19	10	MIM
Por1	YNL055C	Mitochondrial porin (voltage-dependent anion channel)	30	18	11	MOM ^f

Table 1. Continued

Protein Name	Open Reading Frame Name	Description	Molecular Weight (kDa)	Total no. of Identified Spectra		Location ^a
				+UV	–UV	
Hht1,2	YBR010W,YNL031C	Two identical histone H3 proteins	15	3	2	N
Kgd1	YIL125W	Component of the mitochondrial alpha-ketoglutarate dehydrogenase complex	114	11	8	Matrix
Pet9	YBL030C	Major ADP/ATP carrier of the mitochondrial inner membrane	34	16	12	MIM
Atp18	YML081C-A	Subunit of the mitochondrial F1F0 ATP synthase	7	4	3	MIM
Kgd2	YDR148C	Dihydrolipoyl transsuccinylase, a component of the mitochondrial alpha-ketoglutarate dehydrogenase complex	50	12	11	Matrix
Sdh1	YKL148C	Flavoprotein subunit of succinate dehydrogenase	70	6	6	MIM
Sdh2	YLL041C	Iron-sulfur protein subunit of succinate dehydrogenase	30	3	3	MIM
Hsp60	YLR259C	Tetradecameric mitochondrial chaperonin	61	3	3	M
Qcr7	YDR529C	Subunit 7 of the ubiquinol cytochrome c reductase complex	15	2	2	MIM
Atp7	YKL016C	Subunit d of the stator stalk of mitochondrial F1F0 ATP synthase	20	2	2	MIM
—	YEL025C	SWI/SNF and RSC interacting protein 1	136	11	13	N, CP ^g
Mir1	YJR077C	Mitochondrial phosphate carrier, imports inorganic phosphate into mitochondria	33	4	5	M
Cox9	YDL067C	Subunit VIIa of cytochrome c oxidase	7	2	3	MIM
Aco1	YLR304C	Aconitase, required for the tricarboxylic acid cycle and mitochondrial genome maintenance	85	2	3	Matrix
Atp4	YPL078C	Subunit b of the stator stalk of mitochondrial F1F0 ATP synthase	27	2	4	MIM
Htb1,Htb2	YDR224C,YBL002W	Nearly identical histone H2B subtypes	14	1	2	N
Ssc1	YJR045C	Mitochondrial matrix ATPase that is a subunit of the presequence translocase-associated protein import motor	71	1	5	MIM
Rpl13a,b	YDL082W, YMR142C	Protein components of the large (60S) ribosomal subunit	23	—	2	CP

Samples corresponding to the samples shown in lanes 1 (+UV) and 3 (–UV) of Figure 6 were incubated with neutravidin beads. Biotinylated proteins were eluted by heating in SDS-PAGE sample buffer, separated on gel, digested, and subjected to LC-MS/MS analysis. The total number of identified spectra as detected for each protein in two independent experiments is shown. Proteins are ranked in decreasing order of the ratio of the number of identified spectra with / without photo-activation and sorted into groups, separated by horizontal lines, with a ratio ≥ 2 , $1 < \text{ratio} < 2$, and ratio ≤ 1 . The number of spectra for proteins detected at less than 99.0% probability in one of the two conditions is given in italics.

^a Localization according to SGD (*Saccharomyces* genome database).

^b M represents mitochondrial.

^c Matrix represents mitochondrial matrix.

^d N represents nucleus.

^e MIM represents mitochondrial inner membrane.

^f MOM represents mitochondrial outer membrane.

^g CP represents cytoplasm.

caused by some crosslinking occurring in the dark or by aspecific binding of the more hydrophobic benzophenone moiety to membrane proteins. In addition, benzophenone-PC was found to preferentially crosslink to abundant proteins that were also stained by Coomassie, whereas phenylazide-PC demonstrated crosslinking to numerous proteins, mainly of low molecular weight, that were not visible after Coomassie staining. In view of the above, we argue that phenylazide-PC is the preferred, more specific crosslinker to be used in the biological system described in this research. However, depending on the lipid of interest, type of biological membrane, and location of the photo-

activatable moiety in the lipid structure, the benzophenone moiety could be an excellent alternative because of its high chemical stability and high selectivity even in the presence of water and strong nucleophiles (Dorman and Prestwich, 1994).

Several proteins crosslinked by phenylazide-PC and benzophenone-PC have been described to interact with PC or PC-analogs in mitochondrial inner membranes. For example, the crystal structure of the *S. cerevisiae* ubiquinol-cytochrome c reductase complex (cytochrome *bc*₁ complex) contains two tightly bound PC molecules (Lange et al., 2001; Palsdottir et al., 2003) interacting with the subunits Cor1p, Cobp, and Cyt1p. Of

these proteins, Cor1p and Cyt1p were found to be crosslinked by phenylazide-PC and benzophenone-PC. Cobp was not found, possibly because its highly hydrophobic nature might interfere with detection by LC-MS/MS analysis. With the possible exception of Qcr2p, which showed an increase in the number of identified spectra just below the threshold after crosslinking, no other subunits of the cytochrome *bc*₁ complex were found to be crosslinked by phenylazide-PC, indicating high specificity of the phenylazide-PC probe for PC binding pockets. Benzophenone-PC did crosslink to additional subunits of the complex, including Qcr2p. One PC molecule has been found in the crystal structure of bovine heart cytochrome *c* oxidase at a position next to subunits II and VIc (Shinzawa-Itoh et al., 2007). Although the structure of yeast cytochrome *c* oxidase might differ, phenylazide-PC was found to crosslink subunit II, Cox2p, in the present study.

Another mitochondrial protein, glycerol-3-phosphate dehydrogenase (Gut2p), has previously been described to be crosslinked by TID-PC (Janssen et al., 2002), a PC analog with the photoactivatable moiety attached to one of the acyl chains. Recently, Gut2p was shown to be a peripheral membrane protein that was carbonate-wash sensitive and to depend on PC for efficient functioning (Rijken et al., 2007). Interestingly, phenylazide-PC and benzophenone-PC were able to crosslink Gut2p, confirming the interaction of this protein with PC, irrespective of the nature of the photoactivatable moiety and its position on the headgroup. Therefore, the new lipid-crosslinkers appear to be successful in crosslinking peripheral membrane proteins.

Proteins that were not previously described to interact with PC include the two subunits of the peripheral part of the F₁F₀ ATP synthase, Atp1p and Atp2p, which were crosslinked by phenylazide-PC. Also new PC-interacting proteins were identified that have not previously been described as membrane proteins in *S. cerevisiae* or whose membrane association is still disputed. Two components of the pyruvate dehydrogenase complex, Lpd1p and Lat1p, were found to be crosslinked by both probes. Lpd1p also serves as subunit of the homologous 2-oxoglutarate dehydrogenase complex. Both complexes function in the tricarboxylic acid cycle in the mitochondrial matrix. Although in bacteria they are recovered in the soluble cytoplasmic fraction, they were found to be associated with the mitochondrial inner membrane in plants (Millar et al., 1999) and mammals (Maas and Bisswanger, 1990), requiring detergents for solubilization. It was speculated that this association might occur through complex I (Millar et al., 1999), but this complex is not present in *S. cerevisiae*. Therefore, association of these complexes to the mitochondrial inner membrane through lipid-protein interactions might provide an alternative explanation. Other likely peripheral membrane proteins that were crosslinked by phenylazide-PC include the NADH:ubiquinone oxidoreductases Ndi1p and Nde1p, which transfer electrons from NADH to quinones and have been proposed to bind to the membrane through an amphipathic helix (Melo et al., 2004). Mrp7p, which is part of the large subunit of mitochondrial ribosomes, was also found to be crosslinked, consistent with the previously observed membrane association of mitochondrial ribosomes (Jia et al., 2003; Szyrach et al., 2003). A last example of a potential peripheral membrane protein is Ald4p, an aldehyde dehydrogenase that converts acetaldehyde to acetate and is required for growth on ethanol.

Most proteins in Table 1 are present at high copy numbers in the mitochondrial inner membrane. The relative lack of low copy number proteins is probably related to the difficulty of detecting them in an LC-MS/MS approach. However, lowly expressed proteins are crosslinked by phenylazide-PC, considering the difference between the fluorescence signal and Coomassie stain obtained after crosslinking with this probe. The highly abundant ADP/ATP carrier Pet9p does not show a significant increase in the number of identified spectra upon photoactivation of phenylazide-PC (Table 1), demonstrating that the probe does not specifically crosslink abundant proteins.

The carbonate wash resistance of the crosslinked peripheral membrane proteins described above is consistent with the observation that fluorescently labeled crosslink products were carbonate wash-resistant. This indicates that the short azide-containing acyl chains of the probes, which allow for the incorporation of the lipid analogs in the biological membrane by addition from an ethanol solution, were sufficient to anchor peripheral proteins to the membrane. The probes are most likely able to flip-flop across the membrane based on the finding that peripheral proteins from both the matrix and the intermembrane space side of the membrane were crosslinked. This is consistent with the previous finding that externally added spin-labeled PC analogs rapidly redistribute over the two leaflets of the inner mitochondrial membrane (Gallet et al., 1999).

There was little overlap between the crosslink candidates found for ASA-DLPE (1) (Gubbens et al., 2007) and the proteins crosslinked to phenylazide-PC found in the present study, with Gut2p and Cyt1p as exceptions. Because ASA-DLPE and phenylazide-PC have an almost identical photoactivatable moiety, the most likely explanation for these observations is the different headgroup structure of the lipid analogs: ASA-DLPE carries a net negative charge, whereas phenylazide-PC has a zwitterionic headgroup similar to PC. Binding sites of PC have been found to differ from binding sites of negatively charged phospholipids in that the latter contain more polar and positively charged residues, absent in PC binding pockets so as to accommodate the bulky and positively charged choline moiety (Palsdottir and Hunte, 2004). In support of this view, in LUVETs, the PC-analogs used in this study did not crosslink to holo-cytochrome *c*, which interacts electrostatically with anionic lipids (data not shown). The partial overlap observed between the subsets of proteins crosslinked by phenylazide-PC and benzophenone-PC, indicating that these probes target similar sites, in combination with the ASA-DLPE data, suggests that the phospholipid headgroup structure and charge are more important than the nature of the photoactivatable moiety. More information about specific lipid-protein interactions will have to be obtained to characterize the lipid binding motifs involved.

In summary, the new lipid analogs developed in this study allow for the straightforward detection and identification of the lipid headgroup-interacting proteome. Phenylazide-PC was found to be the most suitable photoactivatable lipid for this purpose. It crosslinks to both established interaction partners of PC and possible new interaction partners in IMV, regardless of whether they are peripheral or integral membrane proteins. In addition, new peripheral membrane proteins, not previously described as membrane associated, were identified.

SIGNIFICANCE

Here, a new proteomics approach is described to identify proteins interacting with phospholipid headgroups at the membrane interface. Different analogs of phosphatidylcholine, an abundant phospholipid in eukaryotes, were synthesized from the commercially available precursor *sn*-glycerophosphocholine, thus allowing the addition of custom acyl chains, containing azides for click chemistry, and the addition of different photoactivatable moieties to the quaternary ammonium group of phosphatidylcholine. The probes were validated in a model membrane system in which they were found to render the peripheral membrane protein apo-cytochrome *c* carbonate wash-resistant, as described previously for the photoactivatable probe ASA-DLPE (Gubbens et al., 2007). Photocrosslinking was performed in situ in the inner mitochondrial membrane from *S. cerevisiae* after adding the probes from an ethanol solution. The system was solubilized to attach a reporter molecule containing a terminal alkyne to crosslink products via click chemistry. Lipid analogs containing benzophenone and phenylazide as photoactivatable moieties crosslinked to specific, partially overlapping subsets of proteins as detected by a fluorescent reporter. Compared with phenylazide, benzophenone gave rise to a higher background signal in the absence of photocrosslinking. The crosslink products were biotinylated via click chemistry and purified on neutravidin beads. Mass spectrometry analysis of crosslinked proteins identified both established and potential new interaction partners of phosphatidylcholine, and confirmed the partial overlap in the subsets of proteins crosslinked by both probes. Established interaction partners included protein subunits adjacent to this lipid in the crystal structure of membrane protein complexes, in agreement with the existence of phosphatidylcholine binding pockets. New interaction partners included proteins not previously described as membrane proteins in yeast, and which might be attached peripherally to the mitochondrial inner membrane. These results demonstrate the high potential of our approach to identify a phospholipid-interacting proteome. In principle, the method can be extended to any membrane or any lipid.

EXPERIMENTAL PROCEDURES

Materials

All solvents were distilled before use or were high-pressure liquid chromatography grade. Anhydrous solvents were obtained by storing the solvents over activated 4 Å molecular sieves. BOP (benzotriazol-1-yl-oxy-tris(dimethylamino)phosphonium hexafluorophosphate) was purchased from GL Biochem (Shanghai, China). *sn*-Glycero-3-phosphocholine was purchased from Brunswig Chemie (Amsterdam, the Netherlands). Horse heart cytochrome *c* was purchased from Sigma (St. Louis, MO). Apocytocrome *c* was derived from cytochrome *c* by removing the heme group, as described elsewhere (Fisher et al., 1973), and stored in small aliquots (7.2 mg/ml) in Na₂HPO₄ buffer (10 mM, pH 7.3) at -20°C. DOPC, DOPG, and DLPE were from Avanti Polar Lipids (Alabaster, AL). Photoactivatable probes were stored at a concentration of 5 mM in a 2:1 chloroform/methanol (v/v) solution shielded from light at -20°C. IMVs from *S. cerevisiae* were isolated as described previously (Gubbens et al., 2007) from the wild-type strain BY4742 (*MATα his3Δ1 leu2Δ0 lys2Δ0 ura3Δ0*), and stored in aliquots at -80°C at a protein concentration of approximately 4 mg/ml in H/K buffer (10 mM KCl, 2.5 mM EDTA

(ethylenediaminetetraacetic acid), 5 mM HEPES (4-[2-hydroxyethyl]-*N*'-piperazineethanesulfonic acid) (pH 7.4). TLC plates (silica gel 60F₂₅₄ on glass) were purchased from Merck (Whitehouse Station, NJ).

General Methods

Microwave experiments were performed in a microwave reactor (Biotage Initiator, Uppsala, Sweden). Visualization of TLC spots was achieved with UV light, by staining with an aqueous KMnO₄ (1%) containing 2% K₂CO₃, or with molybdenum blue spray reagent (Sigma, 1.3% molybdenum oxide in 4.2 M aqueous H₂SO₄). NMR spectra were recorded on a Varian Mercury 300 spectrometer. Chemical shifts were calibrated to tetramethylsilane (¹H, δ = 0.00 ppm), CDCl₃ (¹³C, δ = 77.0 ppm), CFC₃ (¹⁹F, δ = 0.00 ppm), and H₃PO₄ (³¹P, δ = 0.00 ppm). Electrospray mass spectra of synthesized compounds were measured on a Shimadzu LCMS-QP8000 single quadrupole bench-top mass spectrometer, which was operated in the positive ionization mode. Phospholipid and phospholipid-crosslinker concentrations were measured by phosphorous determination (Rouser et al., 1970) after destruction in perchloric acid at 180°C using KH₂PO₄ (0–50 nmol) as a standard. Protein concentrations were determined using the BCA method (Pierce) with 0.1% (w/v) SDS added and bovine serum albumin as a standard. Incorporation of the photoactivatable probes in LUVETs and IMVs was performed under red safety light conditions, and their photoactivation was performed using a Mineralight UVGL-58 UV lamp (UVP Inc., San Gabriel, CA). In gel detection of TAMRA was performed on a Typhoon 9400 imaging system (GE Healthcare Bio-Sciences AB, Uppsala, Sweden) using a 532 nm laser for excitation and a 580 ± 15 nm band-pass filter for emission.

Synthesis

Compounds 2, 8, and 11

See Supplemental Experimental Procedures.

Compound 3

To a solution of **9** (66 mg, 0.10 mmol) in DMF (3 ml) was added 4-(bromomethyl)benzophenone (**10**, 110 mg, 0.40 mmol) and 2,6-lutidine (23 μl, 21 mg, 0.20 mmol). The mixture was heated to 120°C by microwave irradiation for 20 min. TLC analysis indicated full conversion. The solvent was removed in vacuo and the residue was purified by flash chromatography (CHCl₃/MeOH/25% aqueous NH₃ 90:10:1 v/v/v → CHCl₃/MeOH/25% aqueous NH₃ 80:20:1 v/v/v) to give pure **3** (39 mg, 0.046 mmol, 46%) as a slightly yellow wax. *R*_f(CHCl₃/MeOH/25% aqueous NH₃ 80:20:1 v/v/v): 0.43; ¹H NMR (300 MHz, CDCl₃) δ 1.23–1.32 (m, CH₂, 24H), 1.46–1.52 (m, CH₂, 8H), 2.21–2.28 (m, CH₂-CO, 4H), 3.14 (s, N-CH₃, 6H), 3.17–3.24 (m, CH₂-N₃, 4H), 3.64 (t (J 4.4 Hz), N-CH₂-CH₂, 2H), 3.96 (dd (J 6.6 Hz, J 5.8 Hz), O-CH₂, 2H), 4.11 (dd (J 12.1 Hz, J 6.9 Hz), O-CH₂, 1H), 4.32 (m, CH₂-CH₂-O, 2H), 4.37 (dd (J 12.1 Hz, J 3.0 Hz), O-CH₂, 1H), 4.69 (s, benzyl CH₂, 2H), 5.19 (m, CH-O, 1H), 7.49 (t (J 7.4 Hz), arom CH, 2H), 7.62 (t (J 7.4 Hz), arom CH, 1H), 7.73 (d (J 7.4 Hz), arom CH, 2H), 7.75 (d (J 8.5 Hz), arom CH, 2H), 7.84 (d (J 8.5 Hz), arom CH, 2H); ¹³C NMR (75.5 MHz, CD₃OD) δ 26.2, 28.0, 30.0–31.4, 35.1, 35.3, 51.8, 52.6, 60.6, 63.9, 65.1, 65.9, 69.7, 72.0, 129.9, 131.3, 131.7, 133.1, 134.5, 134.7, 138.4, 141.1, 174.8, 175.1, 197.6; ES-MS (50 eV) calcd for C₄₃H₆₆N₇O₉P: 855.47, found: *m/z* [M + H]⁺ 856.95 (100%), [M + Na]⁺ 878.55 (21%).

Compound 4

To a solution of **9** (66 mg, 0.10 mmol) in DMF (3 ml) was added *p*-azidobenzyl bromide (**11**, 85 mg, 0.40 mmol) and 2,6-lutidine (23 μl, 0.20 mmol). The mixture was heated to 120°C by microwave irradiation for 35 min. The solvent was removed in vacuo and the residue was purified by flash chromatography (CHCl₃/MeOH/25% aqueous NH₃ 90:10:1 v/v/v → CHCl₃/MeOH/25% aqueous NH₃ 85:15:1 v/v/v) to give pure **4** (47 mg, 0.060 mmol, 60%) as a colorless wax. *R*_f(CHCl₃/MeOH/25% aqueous NH₃ 80:20:1 v/v/v): 0.42; ¹H NMR (300 MHz, CDCl₃) δ 1.27–1.40 (m, CH₂, 24H), 1.54–1.64 (m, CH₂, 8H), 2.23–2.29 (m, CH₂-CO, 4H), 3.23–3.28 (m, CH₂-N₃, 4H), 3.25 (s, N-CH₃, 6H), 3.89 (m, N-CH₂-CH₂, 2H), 3.95 (m, O-CH₂, 2H), 4.11 (dd (J 12.1 Hz, J 7.4 Hz), O-CH₂, 1H), 4.37 (dd (J 12.1 Hz, J 2.7 Hz), O-CH₂, 1H), 4.42 (m, CH₂-CH₂-O, 2H), 4.86 (s, benzyl CH₂, 2H), 5.19 (m, CH-O, 1H), 7.07 (d (J 8.6 Hz), arom CH, 2H), 7.65 (d (J 8.6 Hz), arom CH, 2H); ¹³C NMR (75.5 MHz, CD₃OD) δ 26.2, 28.0, 30.0–31.4, 35.1, 51.4, 52.7, 60.5, 63.9, 65.1, 65.5, 69.7, 72.0, 121.0, 125.4, 136.2, 144.5, 174.8, 175.1; ES-MS (50 eV) calcd for C₃₆H₆₁N₁₀O₈P: 792.44, found: *m/z* [M + H]⁺ 793.30 (100%).

Compound 9

To a solution of *sn*-glycero-3-phosphocholine (**5**, 1.3 g, 5.0 mmol) in DMF (75 ml), DABCO (3.37 g, 30.0 mmol) was added. The mixture was heated to reflux for 5 hr and the solvent was removed *in vacuo* to give crude *sn*-glycero-3-phospho-*N,N*-dimethylethanolamine (**6**) as a brown oil that was used in the next step without further purification. To a solution of 11-azidoundecanoic acid (**8**, 2.27 g, 10.0 mmol) in dry tetrahydrofuran (THF, 25 ml) CDI (1.78 g, 11.0 mmol) was added. After CO₂ evolution had ceased and the solution became clear, the resulting imidazolide solution was added to a solution of crude **6** (~5.0 mmol) and 4-(*N,N*-dimethylamino)pyridine (DMAP, 122 mg, 0.20 mmol) in DMF (100 mL). The mixture was stirred overnight at room temperature and the solvent was removed *in vacuo*. The crude product was purified by flash chromatography using a gradient: CHCl₃/MeOH/25% aqueous NH₃ 90:10:1 v/v/v → CHCl₃/MeOH/25% aqueous NH₃ 50:50:1 v/v/v as eluents, to give **9** (1.11 g, 1.68 mmol, 34%) as a colorless wax. *R*_f(CHCl₃/MeOH/25% aqueous NH₃ 80:20:1 v/v/v): 0.35; ¹H NMR (300 MHz, CDCl₃) δ 1.15–1.45 (m, CH₂, 24H), 1.55–1.62 (m, CH₂, 8H), 2.29 (t (J 7.4 Hz), CH₂, 2H), 2.31 (t (J 7.4 Hz), CH₂-CO, 2H), 2.87 (s, N-CH₃, 6H), 3.21 (m, N-CH₂-CH₂, 2H), 3.26 (2 × t (J 6.9 Hz), CH₂-N₃, 2 × 2H), 4.03 (dd (J 7.4 Hz, J 5.5 Hz), O-CH₂, 2H), 4.16 (dd (J 11.8 Hz, J 6.6 Hz), O-CH₂, 1H), 4.25 (m, CH₂-CH₂-O, 2H), 4.39 (dd (J 11.8 Hz, J 3.3 Hz), O-CH₂, 1H), 5.25 (m, CH-O, 1H); ¹³C NMR (75.5 MHz, CD₃OD) δ 26.2, 28.0, 30.0–31.4, 35.1, 35.3, 43.8, 44.0, 52.6, 59.4, 60.7, 63.8, 65.2, 72.0, 174.8, 175.1; ES-MS (50 eV) calcd for C₂₉H₅₆N₇O₈P: 661.39, found: *m/z* [M + H]⁺ 662.30 (100%), [M + Na]⁺ 684.80 (8%), [2M + H]⁺ 1323.80 (11%).

Crosslinking in LUVETs

7:3 (mol/mol) DOPC/DOPG LUVETs, containing 4 mol% of either the benzophenone or phenylazide probe or no photoactivatable probe, as indicated, were prepared as described (Gubbens et al., 2007). Crosslinking with apocytocrome c (0.12 mg/ml) was carried out as described (Gubbens et al., 2007) at a lipid concentration of 4 mM. For crosslinking at a wavelength of 254 nm the samples were exposed directly to the UV light for 20 min by removing the caps of the tubes and placing the lamp above the samples. After carbonate washing, the LUVETs were resuspended in H-buffer (50 mM NaCl, 1 mM EDTA, 10 mM HEPES, pH 7.5), and the proteins were precipitated in chloroform/methanol (Wessel and Flugge, 1984). Protein pellets were resolubilized by boiling in SDS-PAGE sample buffer containing dithiothreitol (25 mM) and analyzed by SDS-PAGE using 15% (w/v) acrylamide. Gels were stained with Coomassie brilliant blue.

Crosslinking in Mitochondrial Inner Membrane Vesicles

IMVs corresponding to 200–250 μg protein were thawed and diluted to a total volume of 0.5 ml with H/K-buffer containing PMSF (phenylmethanesulfonyl fluoride, 1 mM). The photoactivatable probe indicated was added from a solution in ethanol (10 μl) to either 75 pmol/μg mitochondrial protein or 15 pmol/μg protein. For mock treatment only ethanol (10 μl) was added. The mixtures were incubated at 37°C for 30 min, immediately chilled on ice and, to remove non-incorporated probe, layered on top of sucrose (0.5 M) in H/K-buffer (500 μl). After centrifugation at 165,000 × *g* for 1 h at 4°C, the pellets were washed in H/K-buffer (200 μl) and centrifuged for 20 min at 200,000 × *g* at 4°C. The IMV pellets were resuspended in H/K-buffer at a protein concentration of 1 mg/ml, split, and either left in the dark or treated with UV light (254 nm) on ice for 20 min. Subsequently, either Na₂CO₃ (100 mM) was added to a final concentration of 40 mM Na₂CO₃ or HEPES/KOH (10 mM, pH 7.4) was added to the same final volume. Both solutions contained KCl (10 mM). After 10 min on ice, samples were centrifuged for 20 min at 355,000 × *g* and 4°C. Pellets were resuspended in Tris (Tris(hydroxymethyl)aminomethane)/HCl (50 mM, 50 μl, pH 8.0) containing SDS (1%, w/v) and used as a substrate for the TAMRA or biotin Click-IT Detection Kit (Invitrogen, Carlsbad, CA) according to the manufacturer's instructions. The resulting labeled protein pellets were stored at –20°C until further analysis.

Detection of Crosslinked Proteins

Protein pellets corresponding to 50 μg of protein were heated to 70°C in XT sample buffer (Bio-Rad, Hercules, CA) supplemented with XT reducing agent (Bio-Rad) for 10 min under vigorous shaking to completely solubilize all proteins. Samples were separated on Criterion XT 4%–12% (w/v) Bis-Tris gels (Bio-Rad) in MES running buffer according to the manufacturer's instruc-

tions. For TAMRA detection, 50 μg protein was used per lane, and for biotin detection, 20 μg protein was used per lane. In case of TAMRA detection, the gels were washed in H₂O and scanned for fluorescence before gel staining with Coomassie brilliant blue. In case of biotin detection, proteins were transferred to a nitrocellulose membrane by western blotting, blocked for 1 h with gelatin (3%, w/v, Bio-Rad) in TBST (50 mM Tris/HCl, 100 mM NaCl, 0.05% [v/v] Tween 20, pH 8.0), incubated for 1 h with neutravidin-HRP (1 μg/ml; Pierce, Rockford, IL) in TBST containing gelatin (0.5%, w/v), and visualized, after washing, using ECL solutions.

Affinity Purification

Protein pellets of biotinylated crosslink products, corresponding to approximately 125 μg protein, were dissolved in Tris/HCl (25 μl, 50 mM, pH 8.0) containing SDS (1%, w/v) by incubating at 70°C for 10 min while shaking. An aliquot of 5 μl was stored as a control sample in SDS-PAGE sample buffer, and the remainder was diluted to obtain a 100 μl solution in TBSS (50 mM Tris/HCl, 100 mM NaCl, 0.2% (w/v) SDS, pH 8.0). Neutravidin agarose beads (30 μL, Pierce) were washed two times in TBSS, the protein solution was added, and the beads were incubated for 2h at 4°C while rotating. The beads were washed three times with TBSS and proteins were eluted in concentrated SDS-PAGE sample buffer (62.5 mM Tris/HCl, 2.5% [w/v] SDS, 10.9% [v/v] glycerol, 50 mM dithiothreitol, Bromophenol Blue, pH 6.8, 28 μl) by heating to 95°C for 10 min. To verify the presence of crosslinked proteins, 7 μl was separated on SDS-PAGE gel and biotinylated proteins were detected on western blot as described above. The remainder of the samples was run on an SDS-PAGE gel using 11% (w/v) acrylamide over a distance of approximately 1.5 cm. After staining with Coomassie brilliant blue, the lanes were excised, and cut in three pieces for analysis by LC-MS/MS.

LC-MS/MS Analysis

The gel pieces were subjected to digestion with trypsin and peptides analyzed by nanoscale LC-MS/MS by coupling an Agilent 1100 Series LC system to a LTQ XL quadrupole ion trap mass spectrometer (Finnigan, San Jose, CA), as described previously (Gubbens et al., 2007). The only modification was that, after digestion, the peptides were extracted using 5% (v/v) formic acid instead of acetic acid. Tandem mass spectra were extracted and charge state deconvoluted by BioWorks (Thermo Scientific, Waltham, MA; version 3.3). All MS/MS samples were analyzed using Mascot (Matrix Science, London, UK; version 2.2.03) and X! Tandem (www.thegpm.org; version 2007.01.01.1), both set up to search the Yeast SGD database (5779 entries) with a parent ion tolerance of 0.5 Da and a fragment ion mass tolerance of 0.9 Da. Fixed and variable modifications were the iodoacetamide derivative of cysteine and oxidation of methionine, respectively. Scaffold (version 01_07_00, Proteome Software, Portland, OR) was used to validate MS/MS based peptide and protein identifications. Peptide identifications were accepted if they could be established at greater than 80.0% probability as specified by the Peptide Prophet algorithm (Keller et al., 2002). Protein identifications were accepted if they could be established at greater than 99.0% probability as specified by the Protein Prophet algorithm (Nesvizhskii et al., 2003) and contained at least two identified peptides in one of the samples. Proteins that contained similar peptides and could not be differentiated based on MS/MS analysis alone were grouped to satisfy the principles of parsimony.

SUPPLEMENTAL DATA

The Supplemental Data include Supplemental Experimental Procedures and two tables and can be found with this article online at [http://www.cell.com/chemistry-biology/supplemental/S1074-5521\(09\)00003-9](http://www.cell.com/chemistry-biology/supplemental/S1074-5521(09)00003-9).

ACKNOWLEDGMENTS

This work was supported by the Netherlands Proteomics Centre.

Received: June 27, 2008
Revised: October 24, 2008
Accepted: November 11, 2008
Published: January 29, 2009

REFERENCES

- Ballell, L., Alink, K.J., Slijper, M., Versluis, C., Liskamp, R.M., and Pieters, R.J. (2005). A new chemical probe for proteomics of carbohydrate-binding proteins. *ChemBioChem* 6, 291–295.
- Berman, A., Shearing, L.N., Ng, K.F., Jinsart, W., Foley, M., and Tilley, L. (1994). Photoaffinity labelling of *Plasmodium falciparum* proteins involved in phospholipid transport. *Mol. Biochem. Parasitol.* 67, 235–243.
- Blonder, J., Conrads, T.P., and Veenstra, T.D. (2004). Characterization and quantitation of membrane proteomes using multidimensional MS-based proteomic technologies. *Expert Rev. Proteomics* 1, 153–163.
- Brunner, J. (1993). New photolabeling and crosslinking methods. *Annu. Rev. Biochem.* 62, 483–514.
- Chan, E.W., Chattopadhyaya, S., Panicker, R.C., Huang, X., and Yao, S.Q. (2004). Developing photoactive affinity probes for proteomic profiling: hydroxamate-based probes for metalloproteases. *J. Am. Chem. Soc.* 126, 14435–14446.
- Delfino, J.M., Schreiber, S.L., and Richards, F.M. (1993). Design, synthesis, and properties of a photoactivatable membrane-spanning phospholipidic probe. *J. Am. Chem. Soc.* 115, 3458–3474.
- Desneves, J., Berman, A., Dynon, K., La Greca, N., Foley, M., and Tilley, L. (1996). Human erythrocyte band 7.2b is preferentially labeled by a photoreactive phospholipid. *Biochem. Biophys. Res. Commun.* 224, 108–114.
- DiNitto, J.P., Cronin, T.C., and Lambright, D.G. (2003). Membrane recognition and targeting by lipid-binding domains. *Sci. STKE* 2003, re16.
- Dorman, G., and Prestwich, G.D. (1994). Benzophenone photophores in biochemistry. *Biochemistry* 33, 5661–5673.
- Fisher, W.R., Taniuchi, H., and Anfinsen, C.B. (1973). On the role of heme in the formation of the structure of cytochrome c. *J. Biol. Chem.* 248, 3188–3195.
- Gallet, P.F., Zachowski, A., Julien, R., Fellmann, P., Devaux, P.F., and Maftah, A. (1999). Transbilayer movement and distribution of spin-labelled phospholipids in the inner mitochondrial membrane. *Biochim. Biophys. Acta* 1418, 61–70.
- Gao, Z., and Bauerlein, E. (1987). Identifying subunits of ATP synthase TF0.F1 in contact with phospholipid head groups, α -subunits are labelled selectively by a new photoreactive phospholipid designed for hydrophilic photolabelling. *FEBS Lett.* 223, 366–370.
- Gubbens, J., Vader, P., Damen, J.M., O'Flaherty, M.C., Slijper, M., de Kruijff, B., and de Kroon, A.I. (2007). Probing the membrane interface-interacting proteome using photoactivatable lipid cross-linkers. *J. Proteome Res.* 6, 1951–1962.
- Hertmetter, A., Stutz, H., Franzmair, R., and Paltauf, F. (1989). 1-O-Tritylsno-glycero-3-phosphocholine: a new intermediate for the facile preparation of mixed-acid 1,2-diacylglycerophosphocholines. *Chem. Phys. Lipids* 50, 57–62.
- Hoja, U., Marthol, S., Hofmann, J., Stegner, S., Schulz, R., Meier, S., Greiner, E., and Schweizer, E. (2004). HFA1 encoding an organelle-specific acetyl-CoA carboxylase controls mitochondrial fatty acid synthesis in *Saccharomyces cerevisiae*. *J. Biol. Chem.* 279, 21779–21786.
- Janssen, M.J., van Voorst, F., Ploeger, G.E., Larsen, P.M., Larsen, M.R., de Kroon, A.I., and de Kruijff, B. (2002). Photolabeling identifies an interaction between phosphatidylcholine and glycerol-3-phosphate dehydrogenase (Gut2p) in yeast mitochondria. *Biochemistry* 41, 5702–5711.
- Jia, L., Dienhart, M., Schrampp, M., McCauley, M., Hell, K., and Stuart, R.A. (2003). Yeast Oxa1 interacts with mitochondrial ribosomes: the importance of the C-terminal region of Oxa1. *EMBO J.* 22, 6438–6447.
- Jordi, W., and De Kruijff, B. (1996). Apo- and holo-cytochrome c-membrane interactions. In *Cytochrome C: A Multidisciplinary Approach*, R.A. Scott and A.G. Mauk, eds. (Sausalito, CA: University Science Books), pp. 449–472.
- Keller, A., Nesvizhskii, A.I., Kolker, E., and Aebersold, R. (2002). Empirical statistical model to estimate the accuracy of peptide identifications made by MS/MS and database search. *Anal. Chem.* 74, 5383–5392.
- Kuhlmann, J., Tebbe, A., Volkert, M., Wagner, M., Uwai, K., and Waldmann, H. (2002). Photoactivatable synthetic Ras proteins: “baits” for the identification of plasma-membrane-bound binding partners of Ras. *Angew. Chem. Int. Ed. Engl.* 41, 2546–2550.
- Lange, C., Nett, J.H., Trumpower, B.L., and Hunte, C. (2001). Specific roles of protein-phospholipid interactions in the yeast cytochrome bc1 complex structure. *EMBO J.* 20, 6591–6600.
- LeKim, D., Heidemann, G., and Betzing, H. (1979). Verfahren zur Demethylierung von cholinhaltigen Phospholipiden. German patent DE 2728893.
- Liu, J., and Tor, Y. (2003). Simple conversion of aromatic amines into azides. *Org. Lett.* 5, 2571–2572.
- Maas, E., and Bisswanger, H. (1990). Localization of the alpha-oxoacid dehydrogenase multienzyme complexes within the mitochondrion. *FEBS Lett.* 277, 189–190.
- Melo, A.M., Bandejas, T.M., and Teixeira, M. (2004). New insights into type II NAD(P)H:quinone oxidoreductases. *Microbiol. Mol. Biol. Rev.* 68, 603–616.
- Millar, A.H., Hill, S.A., and Leaver, C.J. (1999). Plant mitochondrial 2-oxoglutarate dehydrogenase complex: purification and characterization in potato. *Biochem. J.* 343, 327–334.
- Montecucco, C. (1988). Photoreactive lipids for the study of membrane-penetrating toxins. *Methods Enzymol.* 165, 347–357.
- Montecucco, C., Schiavo, G., Gao, Z., Bauerlein, E., Boquet, P., and Das-Gupta, B.R. (1988). Interaction of botulinum and tetanus toxins with the lipid bilayer surface. *Biochem. J.* 251, 379–383.
- Nesvizhskii, A.I., Keller, A., Kolker, E., and Aebersold, R. (2003). A statistical model for identifying proteins by tandem mass spectrometry. *Anal. Chem.* 75, 4646–4658.
- Palsdottir, H., and Hunte, C. (2004). Lipids in membrane protein structures. *Biochim. Biophys. Acta* 1666, 2–18.
- Palsdottir, H., Lojero, C.G., Trumpower, B.L., and Hunte, C. (2003). Structure of the yeast cytochrome bc1 complex with a hydroxyquinone anion Qo site inhibitor bound. *J. Biol. Chem.* 278, 31303–31311.
- Rijken, P.J., De Kruijff, B., and De Kroon, A.I. (2007). Phosphatidylcholine is essential for efficient functioning of the mitochondrial glycerol-3-phosphate dehydrogenase Gut2 in *Saccharomyces cerevisiae*. *Mol. Membr. Biol.* 24, 269–281.
- Rostovtsev, V.V., Green, L.G., Fokin, V.V., and Sharpless, K.B. (2002). A stepwise Huisgen cycloaddition process: copper(I)-catalyzed regioselective “ligation” of azides and terminal alkynes. *Angew. Chem. Int. Ed. Engl.* 41, 2596–2599.
- Rouser, G., Fleischer, S., and Yamamoto, A. (1970). Two dimensional thin layer chromatographic separation of polar lipids and determination of phospholipids by phosphorus analysis of spots. *Lipids* 5, 494–496.
- Salisbury, C.M., and Cravatt, B.F. (2007). Click chemistry-led advances in high content functional proteomics. *QSAR Comb. Sci.* 26, 1229–1238.
- Santoni, V., Molloy, M., and Rabilloud, T. (2000). Membrane proteins and proteomics: un amour impossible? *Electrophoresis* 21, 1054–1070.
- Shinzawa-Itoh, K., Aoyama, H., Muramoto, K., Terada, H., Kurauchi, T., Tadehara, Y., Yamasaki, A., Sugimura, T., Kurono, S., Tsujimoto, K., et al. (2007). Structures and physiological roles of 13 integral lipids of bovine heart cytochrome c oxidase. *EMBO J.* 26, 1713–1725.
- Speers, A.E., and Cravatt, B.F. (2004). Profiling enzyme activities in vivo using click chemistry methods. *Chem. Biol.* 11, 535–546.
- Szyrach, G., Ott, M., Bonnefoy, N., Neupert, W., and Herrmann, J.M. (2003). Ribosome binding to the Oxa1 complex facilitates co-translational protein insertion in mitochondria. *EMBO J.* 22, 6448–6457.
- Thiele, C., Hannah, M.J., Fahrenholz, F., and Huttner, W.B. (2000). Cholesterol binds to synaptophysin and is required for biogenesis of synaptic vesicles. *Nat. Cell Biol.* 2, 42–49.
- Tornøe, C.W., Christensen, C., and Meldal, M. (2002). Peptidotriazoles on solid phase: [1,2,3]-triazoles by regioselective copper(I)-catalyzed

1,3-dipolar cycloadditions of terminal alkynes to azides. *J. Org. Chem.* 67, 3057–3064.

Wallin, E., and von Heijne, G. (1998). Genome-wide analysis of integral membrane proteins from eubacterial, archaean, and eukaryotic organisms. *Protein Sci.* 7, 1029–1038.

Wang, P., Blank, D.H., and Spencer, T.A. (2004). Synthesis of benzophenone-containing analogues of phosphatidylcholine. *J. Org. Chem.* 69, 2693–2702.

Wessel, D., and Flugge, U.I. (1984). A method for the quantitative recovery of protein in dilute solution in the presence of detergents and lipids. *Anal. Biochem.* 138, 141–143.